

# Electric-Field Enhancement of Electron Emission Rates for Deep-Level Traps in n-type GaN

Vladimir P. Markevich,\* Matthew P. Halsall, Lijie Sun, Iain F. Crowe, Anthony R. Peaker, Piotr Kruszewski, Jerzy Plesiewicz, Pawel Prystawko, Sylwester Bulka, and Rafal Jakiela

Results of a deep-level transient spectroscopy (DLTS) study of trapping states in Ni/Au Schottky diodes made on Si-doped GaN layers grown by metal–organic vapor-phase epitaxy (MOVPE) on highly conductive n-type Ammono-GaN substrates are reported. In all as-grown samples, the DLTS signals due to traps with the activation energies for electron emission ( $E_{\text{em}}$ ) of about 0.26 and 0.60 eV (referred to as E1 and E3 traps, respectively) have been detected. It is found that the electric field ( $E$ ) significantly enhances the electron emission rate ( $e_{\text{em}}$ ) for the E1 trap, while for the E3 trap the  $e_{\text{em}}(E)$  dependence is not very strong. The  $e_{\text{em}}(E)$  dependence for the E1 trap is found to be characteristic of attractive traps with spherically symmetric square well potential with a radius of about  $2.9 \pm 0.25$  nm. The  $e_{\text{em}}(E)$  dependence for the E3 trap is accounted for by a phonon-assisted tunneling mechanism. The zero- $E$   $E_{\text{em}}$  values for both traps are determined. Correlations between the concentrations of the E1 and E3 traps and concentrations of impurities (H, C, Si, O, Mg, and Fe) determined by secondary ion mass spectrometry in the samples are investigated. Charge states and origins of the E1 and E3 traps are discussed.

## 1. Introduction

The performance of some GaN-based electronic and optoelectronic devices can be affected by the presence of defects with deep energy levels in the gap.<sup>[1–3]</sup> Therefore, numerous studies of deep-level defects in GaN-based materials and devices with the use of different experimental and modeling techniques have been reported.<sup>[1–5]</sup> However, a comprehensive understanding of deep-level defects in GaN is still missing. A lot of information about the properties of electrically active defects in GaN has been obtained with the use of deep-level transient spectroscopy (DLTS).<sup>[6,7]</sup> Surveys of the detected deep-level traps in nitride materials with their electronic signatures and a discussion of their possible origins have been published.<sup>[1,2]</sup> The majority of DLTS techniques are based on studies of the thermal

emission of carriers from traps in the depletion region of a reverse-biased junction. The electric field ( $E$ ) in the depletion region can significantly increase the emission rates ( $e_{\text{em}}$ ) and should therefore be taken into account upon analysis of DLTS data.<sup>[7]</sup> Important information about the nature of deep-level traps can be obtained from the analysis of the measured  $e_{\text{em}}(E)$  dependencies.<sup>[7–9]</sup> However, the information about the  $e_{\text{em}}(E)$  dependencies for deep-level traps in GaN-based materials is very scarce.<sup>[1,10]</sup> Furthermore, it can be seen from our work that significant variation in the electronic signatures for some deep-level traps in GaN reported in the literature can be explained by the failure to take into account the  $e_{\text{em}}(E)$  dependencies for these traps.


In this work, results of a DLTS study of trapping states in Ni/Au Schottky diodes made on GaN layers grown by metal-organic vapor phase epitaxy (MOVPE) on highly conductive n-type Ammono-GaN substrates are reported. In all the as-grown samples the DLTS signals due to traps with the activation energies for electron emission ( $E_{\text{em}}$ ) of about 0.26 and 0.6 eV (referred to as E1 and E3 traps, respectively) have been detected. With the use of the high-resolution Laplace-DLTS technique,<sup>[11,12]</sup> it has been found that the electric field ( $E$ ) of the reverse-biased junctions significantly enhances electron emission rate ( $e_{\text{em}}$ ) for the E1 trap, while for the E3 trap the  $e_{\text{em}}(E)$  dependence is not very strong. The experimental  $e_{\text{em}}(E)$

V. P. Markevich, M. P. Halsall, L. Sun, I. F. Crowe, A. R. Peaker  
Photon Science Institute and Department of Electrical and Electronic Engineering  
University of Manchester  
Manchester M13 9PL, UK  
E-mail: V.Markevich@manchester.ac.uk

P. Kruszewski, J. Plesiewicz, P. Prystawko  
Institute of High Pressure Physics  
Polish Academy of Sciences  
Sokolowska 29/37, 01-142 Warsaw, Poland

S. Bulka  
Institute of Nuclear Chemistry and Technology  
Dorodna 16, 03-195 Warsaw, Poland

R. Jakiela  
Institute of Physics  
Polish Academy of Sciences  
al. Lotników 32/46, 02-668 Warsaw, Poland

 The ORCID identification number(s) for the author(s) of this article can be found under <https://doi.org/10.1002/pssb.202200545>.

© 2022 The Authors. physica status solidi (b) basic solid state physics published by Wiley-VCH GmbH. This is an open access article under the terms of the Creative Commons Attribution License, which permits use, distribution and reproduction in any medium, provided the original work is properly cited.

DOI: 10.1002/pssb.202200545

dependencies are described analytically and charge states and origins of the E1 and E3 traps are discussed based on the obtained DLTS results, secondary ion mass spectroscopy (SIMS) measurements of concentrations of impurities (H, C, Si, O, Mg, and Fe) in the investigated GaN samples and on the information on these traps available in the published literature.

## 2. Experimental Results

**Figure 1** shows the structures of two wafers (referred to as wafer A and wafer B in the following text), which consist of GaN layers grown by MOVPE on highly-conductive Ammono-GaN substrates at the Institute of High-Pressure Physics of Polish Academy of Sciences.<sup>[13,14]</sup> As it can be seen from Figure 1, the top layer of each wafer was intended to be around 1.5  $\mu\text{m}$  thick and doped with silicon to about  $2.7 \times 10^{16} \text{ cm}^{-3}$ . Samples from these wafers were cut and processed for junction capacitance measurements. The details of growth and

diode processing procedures are described below in the Experimental Section.

**Figure 2** shows current-(density)-voltage ( $J$ - $V$ ) dependencies and spatial profiles of uncompensated donors  $[N_d^+(W)]$  derived from capacitance-voltage ( $C$ - $V$ ) measurements at 300 K for two Schottky diodes on the samples from the different wafers. The good quality of the Schottky diodes allows us to carry out junction capacitance measurements with the application of reverse bias voltage down to  $-20 \text{ V}$  and create a relatively strong electric field (up to  $4 \times 10^5 \text{ V cm}^{-1}$ ) in the depletion region of the reverse-biased diodes.

**Figure 3** shows conventional DLTS spectra recorded for the diodes,  $J$ - $V$  and  $N_d^+(W)$  dependencies of which are shown in Figure 2. Measurement parameters used for the recording of the spectra are given in the graph. The spectra are representative of electron capture/emission events for deep-level traps in regions from about 0.35 to 0.7  $\mu\text{m}$  from the surface. Values of  $2 \times (\Delta C/C_b) \times N_d \times f$  are plotted on the vertical axis in Figure 3, where  $\Delta C$  is the capacitance transient magnitudes,

Sample A	Sample B
1.5 $\mu\text{m}$ n-GaN:Si ( $\sim 2.7 \times 10^{16} \text{ cm}^{-3}$ )	1.5 $\mu\text{m}$ n-GaN:Si ( $\sim 2.7 \times 10^{16} \text{ cm}^{-3}$ )
100 nm GaN:Si ( $5 \times 10^{17} \text{ cm}^{-3}$ )	100 nm GaN:Si ( $5 \times 10^{17} \text{ cm}^{-3}$ )
400 nm GaN:Si ( $2 \times 10^{18} \text{ cm}^{-3}$ )	400 nm GaN:Si ( $2 \times 10^{18} \text{ cm}^{-3}$ )
Ammono-GaN (n-GaN)	50 nm GaN:Si ( $1 \times 10^{19} \text{ cm}^{-3}$ )
	Ammono-GaN (n-GaN)

**Figure 1.** Structure of two wafers with GaN layers grown by metal-organic vapor-phase epitaxy (MOVPE) on highly conductive n-type Ammono-GaN substrates at the Institute of High-Pressure Physics of the Polish Academy of Sciences.

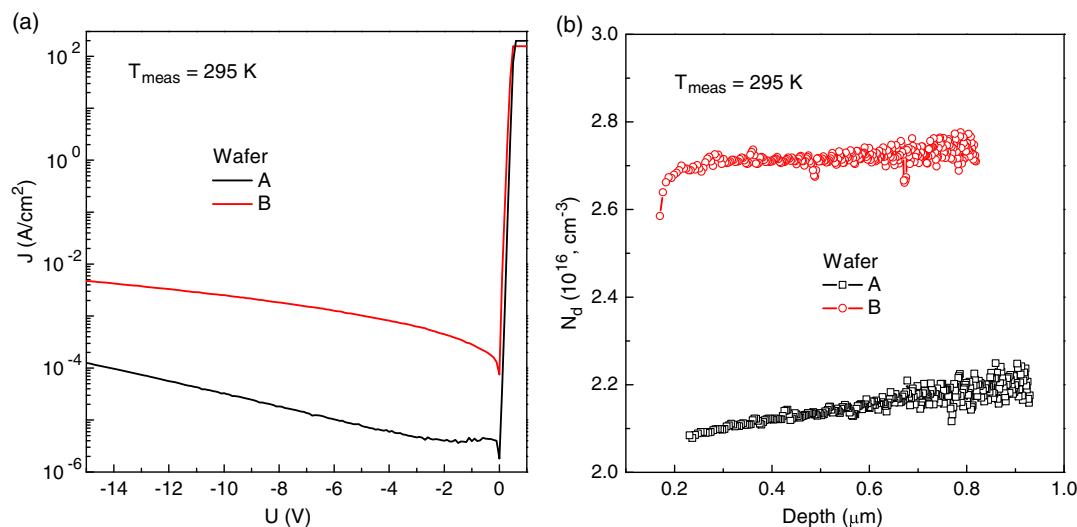


**Figure 2.** a) Current-density-voltage ( $J$ - $V$ ) dependencies and b) spatial profiles of uncompensated donors  $[N_d^+(W)]$  derived from capacitance-voltage ( $C$ - $V$ ) measurements at 300 K for two Schottky diodes on the samples from wafer A and wafer B.

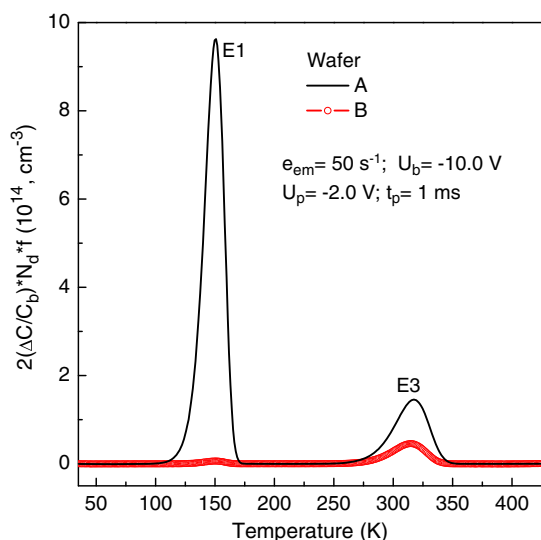


**Figure 3.** Conventional DLTS spectra recorded for two Schottky diodes on the samples from wafer A and wafer B. Measurement parameters used for recording the spectra are given in the graph.

$C_b$  is the capacitance at reverse bias voltage, and  $f$  is the correction function, for calculation of which the widths of the depletion layer at the bias and pulse voltages and the so-called “lambda” layer have been taken into account.<sup>[7,15]</sup> The  $2 \times (\Delta C/C_b) \times N_d \times f$  values at the peak maxima in the DLTS spectra are close to the average trap concentrations in the probed regions. Two electron-emission-related peaks with their maxima at about 150 and 317 K for the DLTS rate window of  $50 \text{ s}^{-1}$  are observed in the recorded spectra. These spectra resemble the DLTS spectra reported in the literature for epi-GaN layers grown on free-standing GaN substrates.<sup>[16–18]</sup> The peaks appearing in the spectra reported in the literature at approximately the same

temperatures as the peaks in the spectra shown in Figure 3 are commonly referred to as E1 and E3 electron traps. We will use this notation for the corresponding peaks seen in the DLTS spectra in Figure 3.

**Figure 4** shows high-resolution Laplace DLTS spectra recorded at the stabilized ( $\pm 2 \text{ mK}$ ) temperatures close to those for the peak maxima of the E1 and E3 traps in the conventional DLTS spectra in Figure 3. The spectra in Figure 4 were measured with the use of the so-called “double” (Laplace)-DLTS technique,<sup>[7,19]</sup> to study the electric-field dependence of electron emission rates ( $e_{em}$ ) for the E1 and E3. The L-DLTS measurements were carried out with the fixed reverse bias voltage ( $U_b$ ) of  $-15 \text{ V}$  and two changeable filling pulse voltages ( $U_{p1}$  and  $U_{p2}$ ). The difference between the filling pulse voltages was kept as  $1 \text{ V}$ , and  $U_{p1}/U_{p2}$  values were changed with either  $0.5$  or  $1 \text{ V}$  increments in the range from  $-1$  to  $-14 \text{ V}$ . This procedure allows us to record and analyze electron-emission-related capacitance transients from relatively narrow probed regions with different values of electric field ( $E$ ). The L-DLTS spectra shown in Figure 4 consist of relatively sharp peaks, the maxima of which shift to higher values of emission rate with increasing  $E$  values for both the E1 and E3 traps. An analysis of the spectra in Figure 4 indicates that i) E1 and E3 emission signals are both related to electron emission from single energy levels of point defects and there is not much heterogeneous strain in the samples [this is evidenced by the shape (sharpness) of a single dominant emission peak in the L-DLTS spectra],<sup>[7,11]</sup> and ii) electron emission rates for both traps are electric-field dependent. It should be further mentioned that the emission rates for the E1 signal as well as for the E3 signal coincide in the L-DLTS spectra for A and B GaN samples if the measurement conditions have been identical. This observation shows that the origins of these emission signals in both GaN samples are identical.

**Figure 5** shows  $e_{em}(E)$  dependencies for the E1 and E3 traps measured at different temperatures. It is found that the electric

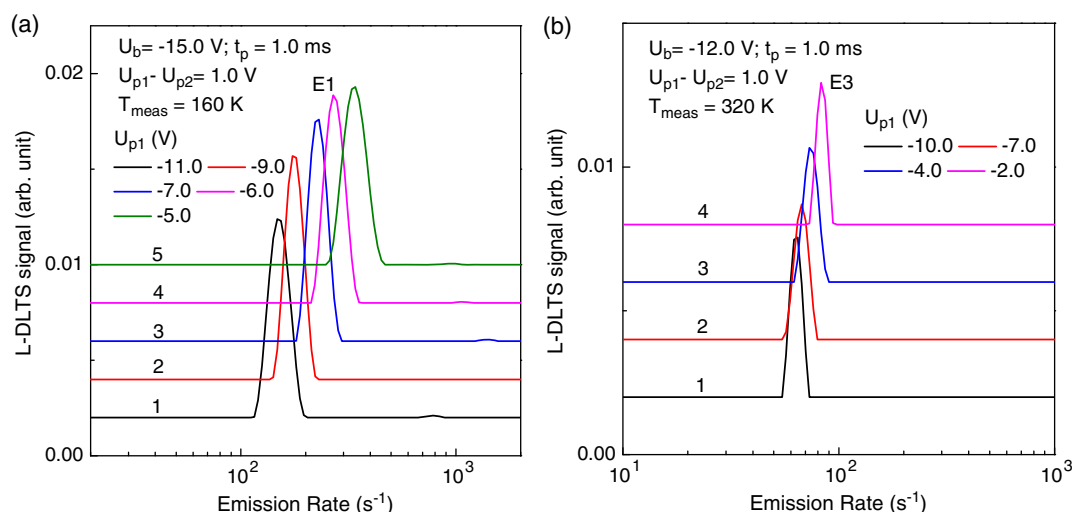


**Figure 4.** Laplace DLTS spectra, which show electron-emission-related signals due to: a) E1 and b) E3 traps in Si-doped GaN layers grown by MOVPE on Ammono-GaN substrates. The spectra were recorded with the use “double” L-DLTS technique with measurement parameters given in the graphs. The spectra are shifted on the vertical axis for clarity.

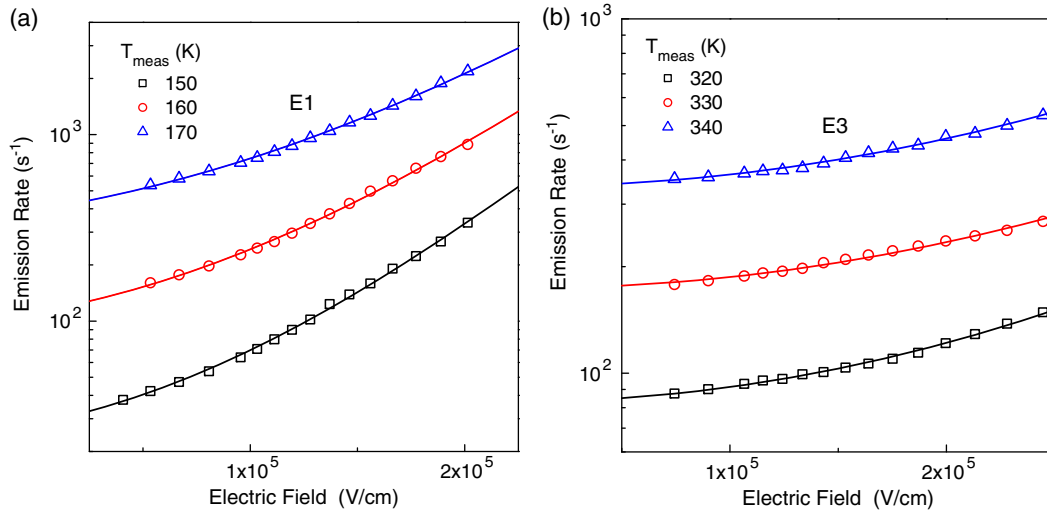


**Figure 5.** Dependencies of electron emission rates versus electric field for: a) E1 and b) E3 traps in Si-doped GaN layers grown by MOVPE on Ammono-GaN substrates. The  $e_{em}(E)$  dependencies were derived from Laplace DLTS spectra measured at different temperatures with the use “double” L-DLTS technique. The solid lines in (a) have been calculated with the use of Equation (2), which describes the  $e_{em}(E)$  dependencies for traps with spherically symmetric square well potential with radius  $R$ . The calculated curves have been fitted to the experimentally measured ones with fitting parameters being  $R$  and zero- $E$   $e_{em}$  values. The solid lines in (b) have been calculated with the use of Equation (1), which describes the  $e_{em}(E)$  dependencies for traps with phonon-assisted tunneling. The calculated curves have been fitted to the experimentally measured ones with fitting parameters being tunneling time  $\tau_2$  and zero- $E$   $e_{em}$  values.

field of the reverse-biased junctions significantly enhances the electron emission rate for the E1 trap, while for the E3 trap the  $e_{em}(E)$  dependence is not very strong. We have attempted to describe the observed dependencies with the use of equations known for the most common mechanisms of electric-field-induced enhancement of carrier emission from deep-level traps. These mechanisms are Poole–Frenkel effect, which occurs for defects with an attractive charge for free carriers, and phonon-assisted tunneling, which works for both charged and neutral defects.<sup>[8,9]</sup> The use of an equation for carrier emission from traps with phonon-assisted tunneling has been successful in fitting to the experimental data for the E3 trap (Figure 5b). The corresponding equation is<sup>[9]</sup>

$$e_{em}/e_{em0} = \exp(E^2/E_{ch}^2) \quad (1)$$

where  $e_{em0}$  is zero- $E$   $e_{em}$  value and the characteristic field  $E_{ch}$  is  $E_{ch} = \sqrt{\frac{3m^*\hbar}{q^2\tau_2^2}}$ , where  $m^*$  is the electron effective mass in GaN,  $\hbar$  is the reduced Planck constant and  $q$  is the value of electron charge. Tunneling time  $\tau_2$  is defined as  $\tau_2 = \frac{\hbar}{2kT} \pm \tau_1$ , with the time constant  $\tau_1$  being of the order of the inverse local impurity vibration frequency and  $k$  is the Boltzmann constant. The calculated curves in Figure 5b) for the E3 trap have been satisfactorily fitted to the experimentally measured ones with tunneling time  $\tau_2$  and  $e_{em0}$  values as the fitting parameters.

However, fitting the experimental data for the E1 trap with the use of equations for 3D Poole–Frenkel effect<sup>[8]</sup> and for phonon-assisted tunneling has not been satisfactory. Instead, it has been found that the experimental  $e_{em}(E)$  dependencies for the E1 trap can be described well by the equation for attractive traps with spherically symmetric square well potential with radius  $R$ . The corresponding equation is<sup>[8]</sup>

$$e_{em}/e_{em0} = (kT/2qER)[\exp(qER/kT) - 1] + 1/2 \quad (2)$$

The calculated curves in Figure 5a have been fitted to the experimentally measured ones with fitting parameters being  $R$  and zero- $E$   $e_{em}$  values. From the fitting of the  $e_{em}(E)$  dependencies measured at different temperatures for the E1 trap, the average fitted value of the  $R$  parameter has been found to be  $2.9 \pm 0.25$  nm.

Figure 6 shows Arrhenius plots of  $T^2$ -corrected electron emission rates for the E1 and E3 derived for  $E = 0$  V cm<sup>−1</sup> from the fitting of the experimental  $e_{em}(E)$  dependencies shown in Figure 5 and measured with the use of double L-DLTS in regions with different  $E$  magnitudes. It can be seen that the electronic signatures (values of activation energy for electron emission ( $\Delta E$ ) and pre-exponential factor ( $A$ )) of the traps derived from the plots are electric-field-dependent. The variation is not very strong for the E3 trap but it is very significant for the E1 trap. For the E1 trap the zero- $E$  value of  $\Delta E$  has been determined as 0.266 eV, however,  $\Delta E$  drops to 0.202 eV for emission rate measurements in the region with  $E = 1.45 \times 10^5$  V cm<sup>−1</sup>. This field dependency is almost certainly the reason for the significant variation in the electronic signatures of the E1 trap in GaN reported in the literature.<sup>[1,2,16–18,20–23]</sup>

### 3. Discussion

The origin of the E1 and E3 traps in GaN materials is still debated in the literature.<sup>[1,2,16–18,20–23]</sup> As has already been mentioned, the analysis of the Laplace DLTS spectra shown in Figure 4 indicate that the E1 and E3 traps in the investigated GaN samples are related to electron emission from single energy levels of point defects.<sup>[7,11]</sup> We consider in the following discussion how the results on the electric-field enhancement of electron emission

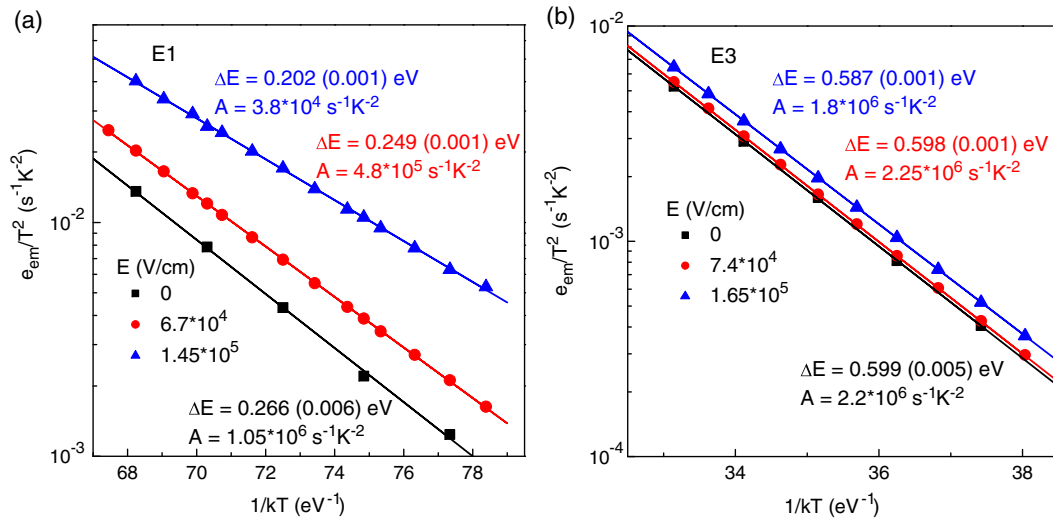


**Figure 6.** Arrhenius plots of  $T^2$ -corrected electron emission rates for the: a) E1 and b) E3 derived for  $E = 0 \text{ V cm}^{-1}$  from the experimental  $e_{\text{em}}(E)$  dependencies shown in Figure 5 and measured with the use of double L-DLTS for regions with different  $E$  magnitudes. The trap electronic signatures (values of activation energy for emission ( $\Delta E$ ) and pre-exponential factor ( $A$ ) derived from the fitting of the plots are given in the graph.

rates and other results obtained in our study are consistent with the identifications of the E1 and E3 traps proposed in the literature.

The results presented in Figure 5b) show that the measured  $e_{\text{em}}(E)$  dependencies for the E3 trap are accounted for by the phonon-assisted tunneling mechanism.<sup>[9]</sup> According to Ref. [9], this mechanism can occur for both charged and neutral (after a carrier emission event) defects. The absence of strong electric-field-induced enhancement of  $e_{\text{em}}$  for the E3 trap indicates that the trap is more likely to be related to an acceptor level of a point defect. The value of the apparent capture cross section for the E3 trap derived from the Arrhenius plot of emission rates at  $E = 0$  (Figure 6b) is found to be about  $2.6 \times 10^{-15} \text{ cm}^2$ , that is consistent with electron capture by neutral defects. We have attempted to carry out direct capture cross-section measurements for the E3 trap by changing the length of the filling pulse ( $t_p$ ) and observed only a very tiny decrease in  $\Delta C$  values upon reducing  $t_p$  from 1 s down to 100 ns. This result is consistent with the point-defect nature of the E3 trap and shows that the lower limit of true capture cross-section value for this trap is about  $1.5 \times 10^{-17} \text{ cm}^2$ . Some strong arguments have been presented recently that the E3 trap is related to an acceptor level of iron atom at the Ga site ( $\text{Fe}_{\text{Ga}}$ ) in GaN.<sup>[18]</sup> The results obtained in our study are consistent with the suggested assignment of the E3 trap to an acceptor level of  $\text{Fe}_{\text{Ga}}$ . The concentration of the E3 traps in our GaN samples varies from a few times of  $10^{13} \text{ cm}^{-3}$  to about  $2 \times 10^{14} \text{ cm}^{-3}$ , while the variation of concentration of Fe atoms determined by SIMS in samples from wafers A and B is in the range from about  $1 \times 10^{14} \text{ cm}^{-3}$  to about  $1 \times 10^{15} \text{ cm}^{-3}$ . [Fe] values in the region measured by DLTS are around  $4.7 \times 10^{14} \text{ cm}^{-3}$  and  $3.2 \times 10^{14} \text{ cm}^{-3}$  in samples from wafers A and B, respectively, as shown in Table 1. These observations support the assignment of the E3 trap to the  $\text{Fe}_{\text{Ga}}(-/0)$  energy level.

The origin of the E1 trap in GaN has been discussed extensively in a recent paper by Kruszewski et al.<sup>[23]</sup> It has been argued

**Table 1.** Concentrations of impurities in the top epitaxial layer of the GaN wafers averaged in the regions from about  $0.25 \mu\text{m}$  to about  $0.8 \mu\text{m}$  from the surface, which have been sampled by DLTS. Chemical concentrations were measured by SIMS and the net electron concentration,  $n$ , was measured by the capacitance–voltage technique. All values are expressed in  $\text{cm}^{-3}$ . Variations in Fe concentration of up to a factor of four were observed as a function of depth and across the samples. The deviations given in the table indicate the spread of values measured by SIMS in the regions probed by DLTS. The error bars related to absolute concentration values are larger.

Impurity/charge carrier	Wafer A	Wafer B
C	$(5.1 \pm 0.3) \times 10^{16}$	$(3.1 \pm 0.3) \times 10^{16}$
Fe	$(4.7 \pm 0.5) \times 10^{14}$	$(3.8 \pm 0.5) \times 10^{14}$
H	$(1.2 \pm 0.05) \times 10^{17}$	$(1.35 \pm 0.1) \times 10^{17}$
Mg	$(4.8 \pm 0.3) \times 10^{14}$	$(2.2 \pm 0.2) \times 10^{15}$
O	$(8.5 \pm 0.2) \times 10^{16}$	$(7.9 \pm 0.2) \times 10^{16}$
Si	$(1.7 \pm 0.1) \times 10^{16}$	$(2.4 \pm 0.3) \times 10^{16}$
$n$	$(2.1 \pm 0.2) \times 10^{16}$	$(2.7 \pm 0.3) \times 10^{16}$

in this article that some point defects could be a potential source of this trap but in summary, it has been mentioned that there is no solid identification of the trap and its structure. Our results confirm the arguments about the point-defect nature of the E1 trap. The results presented in Figure 5a and 6a for the E1 trap show a strong dependence of electron emission rate on electric field values in the probed regions and significant field-induced variation of electronic signatures derived from Arrhenius plots of  $e_{\text{em}}$  values for this trap. The  $e_{\text{em}}(E)$  dependence for the E1 trap is found to be characteristic of an attractive trap (a donor in n-type materials) with spherically symmetric square well potential of  $R$  radius.<sup>[8]</sup> The  $R$ -value for the E1 trap has been determined from the fitting of the  $e_{\text{em}}(E)$  dependence measured at different temperatures as  $2.9 \pm 0.25 \text{ nm}$ . The value of the apparent capture



cross section for the E1 trap derived from the Arrhenius plot of emission rates at  $E=0$  (Figure 6a) is found to be about  $1.3 \times 10^{-15} \text{ cm}^2$ . This value appears to be at the lower limit but still in the range of capture cross-sections of charge carriers by an attractive trap. The measurements of the true capture cross-section for the E1 trap were carried out by changing the length of the filling pulse and, as in the case of the E3 trap, allowed us to estimate only its lower limit, which is about  $2 \times 10^{-17} \text{ cm}^2$ . As it can be seen from Figure 2, the concentration of the E1 trap in a sample from wafer A, which was grown without an introduction of an extra buffer layer (Figure 1) is close to  $1 \times 10^{15} \text{ cm}^{-3}$ , which is more than one order of magnitude higher than the E1 concentration in a sample from wafer B. It has been further found that the concentration of E1 varies in the range from about  $3 \times 10^{14} \text{ cm}^{-3}$  to about  $1.2 \times 10^{15} \text{ cm}^{-3}$  for the diodes at different positions across wafer A. These values seem to be one of the highest for the E1 trap concentration reported in the literature for as-grown GaN samples. It can be speculated that the extra buffer layer in wafer B serves as a barrier for the diffusion of some defects, which are responsible for the formation of the E1 trap, from the Ammono-GaN substrate to the top epi layer. Our attempt to correlate the appearance of the E1 trap in different wafers with concentrations of H, C, Si, O, Mg, and Fe impurities measured by SIMS in the wafers was not very successful. Average concentrations of these impurities determined by SIMS in the regions from about  $0.25 \mu\text{m}$  to about  $0.8 \mu\text{m}$  from the surface are given in Table 1. These regions have been probed in the DLTS measurements. Concentrations of carbon and oxygen impurities are slightly higher in wafer A than in wafer B but it is unlikely that the big difference in concentrations of the E1 trap in the different wafers can be caused by only the observed difference in [C] and [O] values.

With regard to the possible intrinsic (either Ga or N vacancy or interstitial atom) origin of the E1 trap, according to ab-initio calculations,<sup>[4,5]</sup> the first donor level of nitrogen-vacancy ( $V_N$ ) is at about 0.2 eV below the conduction band edge in GaN, which is close to the energy level of the E1 trap as determined from the analysis of DLTS measurements. However, strong arguments have been presented recently that  $V_N$  gives rise to the EE1 electron trap with an energy level at about 0.13 eV below the conduction band edge, the emission signal of which is well separated from the E1-related signal in the DLTS spectra.<sup>[24]</sup> The calculated energy levels of the Ga vacancy and interstitial, and the nitrogen interstitial atom are not consistent with the energy level of the E1 trap.<sup>[4,5]</sup> Summarising the discussion, it is possible that the E1 trap is related to a complex incorporating a native defect and an impurity atom, as was suggested in a number of articles, which have been reviewed in Ref. [23]. However, the structure of the complex and its components are still awaiting a solid identification.

## 4. Conclusion

The results obtained in this study can be considered as evidence of the successful application of the high-resolution Laplace DLTS technique for the characterization of deep-level traps in GaN materials. The application of the L-DLTS technique allows us to obtain some useful information about the properties of two deep-level traps, E1 and E3, which are present in nearly

all as-grown GaN epi layers. First, it has been found from an analysis of the recorded L-DLTS spectra for Si-doped GaN epi layers grown on Ammono-GaN substrates that the E1 and E3 traps are related to single energy levels of point defects and there is no significant strain in the samples. Second, the application of the “double” L-DLTS technique allows us to carry out careful measurements of electric-field dependencies of electron emission rates for both E1 and E3 traps and from an analysis of the experimental  $e_{em}(E)$  dependencies to obtain information about the electronic nature of these traps. It is further shown that significant variation in the electronic signatures for the E1 and E3 traps in GaN reported in the literature can be explained by the failure to take into account the  $e_{em}(E)$  dependencies for these traps. Our results on the E3 trap are consistent with its assignment to an acceptor level of  $\text{Fe}_{\text{Ga}}$ .<sup>[18]</sup> Further studies are necessary for the identification of the E1 trap.

## 5. Experimental Section

Two GaN structures were grown on bulk Ammono-thermal GaN substrates<sup>[13]</sup> of n-type conductivity in close-coupled showerhead (CCS) metal-organic chemical vapor deposition (MOCVD) tool with nearly similar growth conditions, except an introduction of an extra buffer layer for wafer B and slightly higher effective surface temperature and hence reduced growth rate for top epi layer of wafer B.

For wafer B a 50 nm thick layer doped with Si up to  $1 \times 10^{19} \text{ cm}^{-3}$  was grown on an Ammono-GaN substrate. The other two GaN:Si buffer layers of the structures were the same in both samples. The deeper layer was 400 nm thick and doped with silicon to  $2 \times 10^{18} \text{ cm}^{-3}$ , while the shallow one was 100 nm thick and doped to  $5 \times 10^{17} \text{ cm}^{-3}$ . The growth pressure for the top-most GaN:Si layer was 400 torr and the V/III ratio was 670, however, substrate A was more oxygen doped ( $1 \times 10^{19} \text{ cm}^{-3}$ ) and more electrically conductive that resulted in a reduced surface temperature of about  $1020^\circ\text{C}$  as measured by in-situ two-color pyrometer Argus (TM) by Aixtron Ltd. Wafer B was less doped with oxygen ( $7 \times 10^{17} \text{ cm}^{-3}$ ) with the estimated surface temperature of  $T = 1037^\circ\text{C}$ . Ammonia, silane ( $\text{SiH}_4$ ), and TMGa were used as sources of nitrogen, silicon n-type dopant, and gallium, respectively. The difference in effective surface temperatures was responsible for the differences in carbon incorporation as evidenced by SIMS depth profiling (average C concentration according to SIMS measurements is about  $3 \times 10^{16} \text{ cm}^{-3}$  in wafer B and  $(4-5) \times 10^{16} \text{ cm}^{-3}$  in wafer A). It is due to the fact that the higher growth temperature leads to increased methyl radical elimination from the gas phase and reduction of carbon concentration in sample B. Also, the growth rate is lowered due to the gallium desorption at higher temperatures but the silicon doping efficiency is kept high (close to 100%). Therefore, one can see increased silicon concentration in sample B (slightly above  $2 \times 10^{16} \text{ cm}^{-3}$  according to SIMS measurements) in comparison to sample A (slightly below  $2 \times 10^{16} \text{ cm}^{-3}$ ) despite the same  $\text{SiH}_4/\text{TMGa}$  ratio in the gas phase.

Small samples were cut from the wafers and, after cleaning, Schottky barrier diodes were prepared on them by plasma sputtering of Ni/Au and Ti/Al/Ti stacks on the front and back surfaces, respectively. Current-voltage and capacitance-voltage measurements were carried out to assess the quality of the diodes, to determine the concentrations of uncompensated shallow donor atoms, the depth of the depletion region and distribution of electric field in it, and to choose bias voltage and pulse voltages used to probe different regions in electrical measurements. Conventional DLTS and high-resolution Laplace DLTS techniques were used to detect and characterize deep-level traps in the diodes.<sup>[6,7,11]</sup>

## Acknowledgements

The work in the UK was funded by EPSRC via grant EP/TO25131/1. Polish authors would like to thank the National Science Centre, Poland, for

financial support through Project no. 2020/37/B/ST5/02593 and the National Center for Research and Development, Poland, through Project no. WPC/20/DefeGaN/2019.

## Conflict of Interest

The authors declare no conflict of interest.

## Data Availability Statement

The data that support the findings of this study are available from the corresponding author upon reasonable request.

## Keywords

deep levels, deep-level transient spectroscopy, electric field enhancement, GaN, metal-organic vapor phase epitaxy

Received: November 18, 2022

Revised: December 8, 2022

Published online: December 28, 2022

- [1] A. Y. Polyakov, I.-H. Lee, *Mater. Sci. Eng. R* **2015**, 94, 1.
- [2] *Characterization of Defects and Deep Levels for GaN Power Devices* (Eds: T. Narita, T. Kachi), AIP Publishing, Melville, New York **2020**.
- [3] M. Meneghini, C. De Santi, I. Abid, M. Buffolo, M. Cioni, R. A. Khadar, L. Nela, N. Zagni, A. Chini, F. Medjdoub, G. Meneghesso, G. Verzellesi, E. Zanoni, E. Matioli, *J. Appl. Phys.* **2021**, 130, 181101.
- [4] J. L. Lyons, C. G. Van de Walle, *npj Comput. Mater.* **2017**, 3, 12.
- [5] J. L. Lyons, D. Wickramaratne, C. G. Van de Walle, *J. Appl. Phys.* **2021**, 129, 111101.
- [6] D. V. Lang, *J. Appl. Phys.* **1974**, 45, 3023.
- [7] A. R. Peaker, V. P. Markevich, J. Coutinho, *J. Appl. Phys.* **2018**, 123, 161559.
- [8] J. L. Hartke, *J. Appl. Phys.* **1968**, 39, 4871.
- [9] S. D. Ganichev, E. Ziemann, W. Prittl, I. N. Yassievich, A. A. Istratov, E. R. Weber, *Phys. Rev. B - Condens. Matter Mater. Phys.* **2000**, 61, 10361.
- [10] W. Götz, N. M. Johnson, M. D. Bremser, R. F. Davis, *Appl. Phys. Lett.* **1996**, 69, 2379.
- [11] L. Dobaczewski, A. R. Peaker, K. Bonde Nielsen, *J. Appl. Phys.* **2004**, 96, 4689.
- [12] A. R. Peaker, V. P. Markevich, I. D. Hawkins, B. Hamilton, K. Bonde Nielsen, K. Gosinski, *Physica B* **2012**, 407, 3026.
- [13] M. Zajac, R. Kucharski, K. Grabianska, A. Gwardys-Bak, A. Puchalski, D. Wasik, E. Litwin-Staszewska, R. Piotrkowski, J. Z. Domagala, M. Bockowski, *Prog. Cryst. Growth Charact. Mater.* **2018**, 64, 63.
- [14] P. Kruszewski, P. Prystawko, M. Grabowski, T. Sochacki, A. Sidor, M. Bockowski, J. Jasinski, L. Lukasiak, R. Kisiel, M. Leszczynski, *Mater. Sci. Semicond. Process.* **2019**, 96, 132.
- [15] S. Stievenard, D. Vuillaume, *J. Appl. Phys.* **1986**, 60, 973.
- [16] Y. Tokuda, *ECS Trans.* **2016**, 75, 39.
- [17] T. Tanaka, K. Shiojima, T. Mishima, Y. Tokuda, *Jpn. J. Appl. Phys.* **2016**, 55, 061101.
- [18] M. Horita, T. Narita, T. Kachi, J. Suda, *Appl. Phys. Express* **2020**, 13, 071007.
- [19] H. Lefevre, M. Schulz, *Appl. Phys.* **1977**, 12, 45.
- [20] D. C. Look, Z.-Q. Fang, B. Claflin, *J. Cryst. Growth* **2005**, 281, 143.
- [21] A. R. Arehart, A. Corrión, C. Poblenz, J. S. Speck, U. K. Mishra, S. A. Ringel, *Appl. Phys. Lett.* **2008**, 93, 112101.
- [22] A. R. Arehart, A. Corrión, C. Poblenz, J. S. Speck, U. K. Mishra, S. P. Denbaars, S. A. Ringel, *Phys. Status Solidi C* **2008**, 5, 1750.
- [23] P. Kruszewski, P. Kaminski, R. Kozłowski, J. Zelazko, R. Czernecki, M. Leszczynski, A. Turos, *Semicond. Sci. Technol.* **2021**, 36, 035014.
- [24] M. Horita, T. Narita, T. Kachi, J. Suda, *Appl. Phys. Lett.* **2021**, 118, 012106.